Inorganic Chemistry

Article

pubs.acs.org/IC

Singlet and Triplet Energy Transfers in Tetra-(*meso*-truxene)zinc(II)- and Tetra-(*meso*-tritruxene)zinc(II) Porphyrin and Porphyrin-Free Base Dendrimers

Bin Du,[†,‡] Daniel Fortin,[‡] and Pierre D. Harvey*[,†,‡]

[†]Département de Chimie, Université de Sherbrooke, 2500 Boul. de l'Université, Sherbrooke, Québec, Canada

[‡]Institut de Chimie Moléculaire de l'Université de Bourgogne (ICMUBUMR, 5260), Université de Bourgogne, Dijon, France

Supporting Information

ABSTRACT: The synthesis, optical properties, and energy transfer features of four dendrimers composed of *meso*-tetrasubstituted zinc(II) porphyrin (**ZnP**) or a free base (**P**) central core, where the substituents are four truxene (**Tru**) or four tritruxene dendrons (**TriTru**), **TruP**, **TriTruP**, **TruZnP**, and **TriTruZnP**, are reported. Selective excitation of the truxene donors results in a photoinduced singlet energy transfer from the truxenes to the porphyrin acceptor. The rates for singlet energy transfer (k_{ET}), evaluated from the change in the fluorescence lifetime of the donors (**Tru** and **TriTru**) in the presence and absence of the acceptor (**P** or **ZnP**) for **TruP**, **TruZnP**, **TriTruP**, and **TriTruZnP**, are 5.9, 1.2, 0.87, and 0.74 $(ns)^{-1}$ at 298 K and 2.6, 2.6, 2.7, and 1.2 $(ns)^{-1}$ at 77 K, respectively. A slow triplet−triplet energy transfer from truxene to porphyrin cores in glassy 2MeTHF at 77 K is also reported with rates of 1.3×10^3 and 0.10×10^2 s^{-1} for **TruZnP** and **TriTruZnP**, respectively. If the Dexter mechanism for the triplet energy transfers is considered, these slow rates are easily explained by a poor orbital overlap between the truxene and porphyrin π systems. The fluorescence quantum yields (Φ_F) are 0.20 and 0.16 for **TruP** and **TriTruP** and 0.08 and 0.10 for **TruZnP** and **TriTruZnP**, respectively at 298 K. At 298 K, a phosphorescence from **TruZnP** at 795 nm was also observed and is associated with the **ZnP** chromophore.

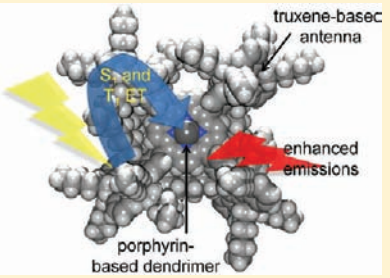

INTRODUCTION

Over the past several decades, the design of rigid π-conjugated porphyrins has been extensivly studied due to their wide application as active components in supramolecular, multichromophoric, and covalently linked assemblies involving energy and electron transfers, as well as in electronic and optoelectronic devices.[1−4]

Truxene, a C_{3h} symmetric polycyclic hydrocarbon, is considered a promising building block in the development of discotic liquid crystals, for enforcing supramolecular organization, and as a potential molecular energy donor.[5−11] Furthermore, facile functionalization in three dimensions allows for larger dendritic structures, making these systems attractive for the investigation of the effects of increasing molecular complexity on photophysical properties, comparing them with those of rigid polyfluorene,[12] polyphenylene,[13] polyphenylacetylene,[14−16] oligo(p-phenylene vinylene),[1] and carbazole.[17] Moreover, recently reported truxene derivatives, including a variety of star-shaped oligomers and dendritic structures with extended π conjugation of the polyaromatic core, as well as truxene-based donor−acceptor systems, exhibit interesting photophysical properties.[18,19] For instance, highly efficient and color-stable deep-blue organic light-emitting diodes based on solution-processable dendrimers constructed with truxene have been reported.[18d]

To the best of our knowledge, only one report, in which a single truxene unit is covalently linked to a porphyrin core (through a benzene bridge), leading to a red emitting species in solution and as a solid film, exists.[20] However, a comprehensive review of the photoinduced energy transfer processes in multichromophoric arrays containing truxenes and porphyrins has not been undertaken. Bearing in mind that multiaryl-containing porphyrins may be useful models for better understanding the antenna processes in photosynthesis[21,22] and may also have potential applications in optoelectronic devices,[1] we now wish to report the synthesis of a series of porphyrins containing truxene or tritruxene directly linked to the porphyrin center at the *meso* positions (Chart 1). The photophysical properties are investigated, focusing on both the singlet and triplet energy transfers from the truxene donors to the central free base or zinc(II) porphyrin core.

EXPERIMENTAL SECTION

Instruments. ^1H and ^{13}C NMR spectra were collected on a Bruker DRX 300 or 400 spectrometer in deuterated chloroform solutions, with tetramethylsilane (TMS) as the internal standard. MALDI-TOF mass spectra were recorded on a Bruker BIFLEX III TOF mass spectrometer (Bruker Daltonics, Billerica, MA, U.S.A.) using a 337 nm nitrogen laser with dithranol as a matrix. Elemental analyses were carried out using an Elementar Vario EL (Germany). The molecular weights of the polymers were determined by GPC (HP 1050 series HPLC with visible wavelength and fluorescence detectors)

Received: June 25, 2011
Published: October 21, 2011

Chart 1

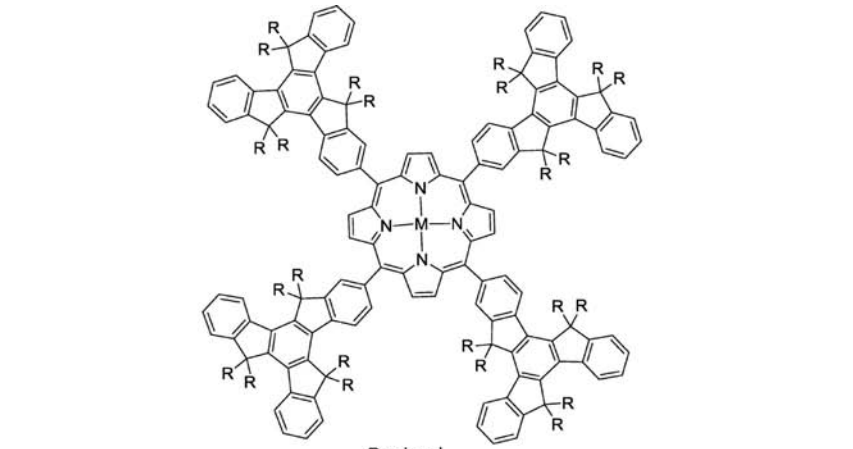

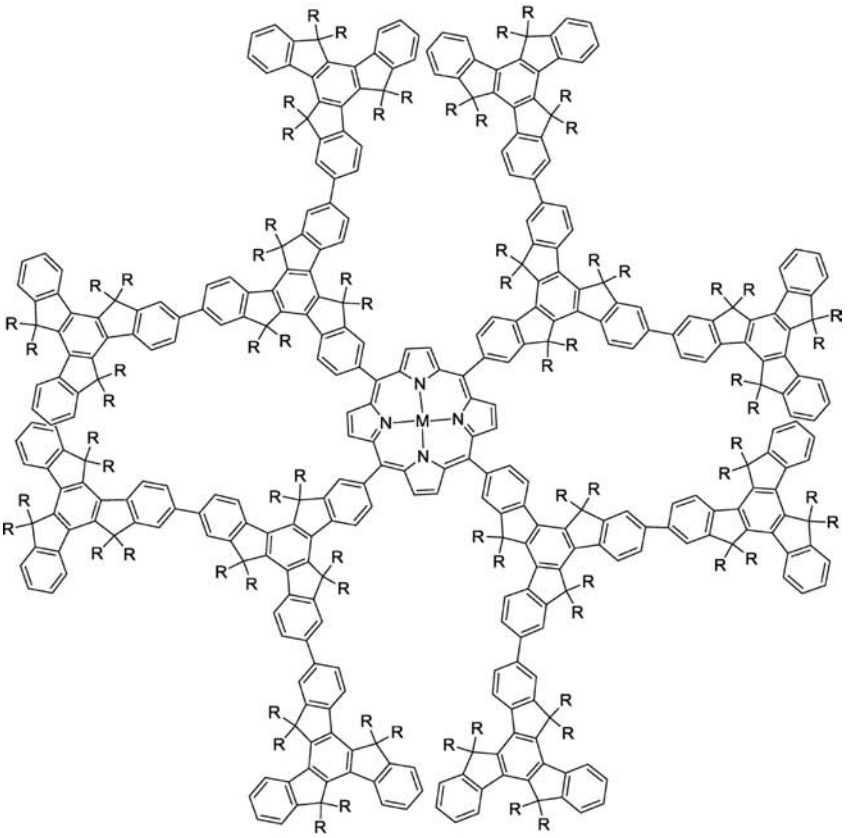

using polystyrene standards and THF as the eluent. UV−vis spectra were recorded on a Hewlett-Packard diode array model 8452A. Emission and excitation spectra were obtained using a double monochromator Fluorolog 2 instrument from Spex. Fluorescence and phosphorescence lifetimes were measured on a Timemaster Model TM-3/2003 apparatus from PTI, incorporating a nitrogen laser as the source and a high-resolution dye laser (fwhm = 1.4 ns). Fluorescence lifetimes were obtained from high-quality decays and deconvolution or distribution lifetime analysis. The uncertainties ranged from 20 to 40 ps on the basis of multiple measurements. Phosphorescence lifetimes were determined using a PTI LS-100 incorporating a 1 μs tungsten flash lamp (fwhm ~ 1 μs). Flash photolysis spectra and transient lifetimes were measured using a Luzchem spectrometer using the 355 nm line of a YAG laser from Continuum (Serulite; fwhm =13 ns).

Quantum Yield Measurements. For measurements at 298 K, all samples were prepared in a glovebox, under argon (O_2 < 12 ppm), by dissolution of the compounds in 2MeTHF, using 1 cm^3 quartz cells with a septum. Three different measurements (i.e., different solutions) were performed for each set of photophysical data (quantum yield). The sample concentrations were chosen to correspond to an absorbance of 0.05 at the excitation wavelength. Each absorbance value was measured five times for better accuracy in the measurements

dx.doi.org/10.1021/ic2013667 | Inorg. Chem. 2011, 50, 11493–11505

of emission quantum yield. The references were tetraphenylporphyrin (0.10 in THF)[2b] or tetraphenylporphyrin zinc(II) (0.033 in THF).[23]

Theoretical Computations. Calculations were performed using Gaussian 09(1)[24] at the Université de Sherbrooke on the Mammouth supercomputer supported by le Réseau Québécois de Calculs de Haute Performances. The entire structure was optimized using the ONIOM layers B3LYP[25]/3-21 g*:[26] PM6[27] method. The high layer geometry was then utilized to perform the final DFT[28] and TDDFT[29] calculations. The calculated absorption spectra and related MO contributions were obtained from the TDDFT/Singlets output file and gausssum 2.1.[30]

Synthesis. Chemicals were purchased from Aldrich or Acros and used as received. 2-Bromo-5,5′,10,10′,15,15′-hexahexyltruxene (**1**), **2**-boronic acid, and 5,5′,10,10′,15,15′-hexa-hexyltruxene (**4**) were prepared as detailed in the literature.[31]

*2-Carbaldehyde-5,5′,10,10′,15,15′-hexahexyltruxene (**2**).* A solution of *n*-BuLi (20.0 mmol) in hexane was added dropwise to a solution of **1** (9.26 g, 10.0 mmol) in 250 mL of anhydrous Et_2O at −78 °C. After 0.5 h, the mixture was warmed to room temperature and kept for an additional 0.5 h. The mixture was recooled to −78 °C, and anhydrous DMF (1.46 g, 20.0 mmol) was added slowly. The solution was left overnight, and dilute HCl (1 N, 15 mL) was added slowly, with stirring, over a period of 1 h. The reaction mixture was transferred to an extraction funnel and extracted with 3 successive aliquots of Et_2O. The combined organic extracts were washed with water and brine and dried over $MgSO_4$. After the solvent was removed under reduced pressure, the residue was purified by column chromatography using dichloromethane and pentane (1:8) as a solvent to afford **2** as a white solid (4.80 g, 55%). ^{1}H NMR ($CDCl_3$, 300 MHz, ppm): δ 10.13 (1H, s), 8.54−8.52 (1H, d, J = 8 Hz), 8.38−8.35 (2H, m), 8.01−7.90 (2H, m), 7.48−7.26 (6H, m), 3.00−2.86 (6H, m), 2.16−2.04 (6H, m), 0.88−0.47 (66H, m). ^{13}C NMR ($CDCl_3$, 75 MHz, ppm): δ 192.4, 154.6, 153.6, 153.5, 146.9, 146.7, 146.1, 139.9, 139.8, 138.8, 137.0, 134.4, 129.3, 126.8, 126.2, 124.8, 124.7, 122.3, 122.2, 55.9, 55.8, 37.2, 36.9, 36.7, 31.5, 29.5, 29.4, 23.9, 22.3, 13.9. MALDI-TOF MS, m/z calcd for $C_{64}H_{90}O$: 874.70. Found (MH^+): 875.435. Elem anal. calcd (%) for $C_{64}H_{90}O$: C, 87.81; H, 10.36; Found: C, 88.19; H, 9.97.

*2-Carbaldehyde-7,12-dibromo-5,5′,10,10′,15,15′-hexahexyltruxene (**3**/TruCHO).* A solution of bromine (2.10 mL, 40.0 mmol) in 10 mL of chloroform was added dropwise to a mixture of **2** (8.75 g, 10.0 mmol) and 20 mg of anhydrous $FeCl_3$ (as catalyst) in 60 mL of chloroform at 0 °C over 1 h. The reaction was then warmed to room temperature. After stirring for 24 h, the mixture was washed with a saturated sodium thiosulfate solution and brine to remove the excess bromine. The precipitate was filtered and washed with water three times. The filtrate was washed with brine and extracted with chloroform. The removal of the solvent gave a yellow residue. Recrystallization of the combined solid from EtOH afforded **3** as a white solid (9.80 g, 96%). ^{1}H NMR ($CDCl_3$, 300 MHz, ppm): δ 10.10 (1H, s), 8.47−8.45 (1H, d, J = 8.4 Hz), 8.19−8.15 (2H, m), 7.96−7.87 (2H, m), 7.56−7.48 (4H, m), 2.87−2.81 (6H, m), 2.05−1.52 (6H, m), 0.92−0.74 (36H, m), 0.60−0.54 (18H, m), 0.46−0.39 (12H, m). ^{13}C NMR ($CDCl_3$, 75 MHz, ppm): δ 192.3, 155.8, 154.4, 146.6, 146.2, 146.1, 138.6, 138.0, 137.3, 134.7, 129.5, 126.0, 125.6, 124.8, 122.3, 121.3, 56.2, 55.9, 37.0, 36.8, 36.7, 41.5, 29.4, 23.9, 22.3, 13.9. MALDI-TOF MS, m/z calcd for $C_{64}H_{88}Br_2O$: 1030.52. Found (MH^+): 1031.425. Elem anal. calcd (%) for $C_{64}H_{88}Br_2O$: C, 74.40; H, 8.58; Found: C, 74.28; H, 8.45.

*2-Carbaldehyde-7,12-di(5,5′,10,10′,15,15′-hexahexyltruxene)-5,5′,10,10′,15,15′-hexahexyl -truxene (**5**/TriTruCHO).* $Pd(PPh_3)_4$ (0.29 g, 0.26 mmol) was added to a mixture of **3** (10.3 g, 10.0 mmol), **4** (27.0 g, 30.0 mmol), and Na_2CO_3 (16 mL, 2.0 mol/L in water) in tetrahydrofuran (THF). After degassing the solution, the mixture was refluxed overnight and then quenched with an aqueous NH_4Cl solution. The aqueous layer was extracted twice with CH_2Cl_2, and the combined organic layers were washed with brine and dried over Na_2SO_4. The solvent was removed under vacuum conditions, leaving a white residue. The crude product was purified by column chromatography on silica gel with hexane/EtOAc (10:1) to give, after removal of the solvent, a white solid (15.4 g, 60%). ^{1}H NMR ($CDCl_3$, 300 MHz, ppm): δ 10.26 (1H, s), 8.59−8.49 (5H, m), 8.40−8.37 (4H, m), 8.03 (1H, s), 7.95−7.92 (1H, m), 7.83−7.82 (8H, m), 7.48−7.32 (12H, m), 3.04−2.97 (18H, m), 2.17−2.06 (18H, m), 0.88−0.52 (198H, m). ^{13}C NMR ($CDCl_3$, 75 MHz, ppm): δ 192.7, 154.8, 154.6, 154.5, 153.9, 153.8, 145.1, 140.6, 134.7, 126.3, 125.5, 125.3, 122.4, 120.5, 56.4, 56.3, 56.1, 55.9, 37.3, 37.2, 31.8, 31.8, 31.8, 29.9, 29.8, 24.3, 24.2, 22.6, 22.6, 14.2. MALDI-TOF MS, m/z calcd for $C_{190}H_{266}O$ m/z: 2564.08. Found: 2480.395 (M-$(CH_2)_5CH_3$) $^+$, 2536.449 (M-CH_2CH_3)$^+$. Elem anal. calcd (%) for $C_{190}H_{266}O$: C, 88.93; H, 10.45; Found: C, 88.68; H, 10.76.

*7,12-Dibromo-5,5′,10,10′,15,15′-hexahexyltruxene (**6**).* A solution of bromine (1.20 mL, 23.0 mmol) in 10 mL of chloroform was added dropwise to a mixture of 5,5,10,10,15,15-hexyltruxene (10.0 g, 11.8 mmol) in 60 mL of chloroform at 0 °C over 1 h. The reaction was warmed to room temperature and stirred for 24 h. The mixture was washed with a saturated sodium thiosulfate solution and brine. Removal of the solvent gave a yellow solid. Recrystallization from EtOH afforded a white solid (9.40 g, 80%). ^{1}H NMR ($CDCl_3$, 300 MHz, ppm): δ 8.37−8.30 (1H, m), 8.22−8.16 (2H, m), 7.56−7.26 (7H, m), 2.98−2.80 (6H, m), 2.07−1.94 (6H, m), 0.83−0.50 (66H, m). ^{13}C NMR ($CDCl_3$, 75 MHz, ppm): δ 156.3, 156.1, 153.6, 145.6, 145.1, 144.6, 139.3, 138.9, 137.8, 137.6, 129.6, 129.5, 124.8, 122.5, 121.0, 56.2, 56.1, 55.9, 37.15, 37.1, 37.0, 31.7, 29.9, 29.7, 29.6, 24.1, 22.5, 14.1. Elem anal. calcd (%) for $C_{63}H_{88}Br_2$: C,75.28; H, 8.82; N, 1.52. Found: C, 75.78; H, 9.21.

*7,12-Di(5,5′,10,10′,15,15′-hexahexyltruxene)-5,5′,10,10′,15,15′-hexahexyltruxene (**7**/TriTru).* $Pd(PPh_3)_4$ (0.11 g, 0.10 mmol) was added to a mixture of **6** (3.0 g, 3.0 mmol), **4** (2.7 g, 3.0 mmol), and KOH (12 mL, 2.0 mol/L in distilled water) in THF (10 mL). After degassing the solution, the mixture was refluxed overnight and quenched with an aqueous NH_4Cl solution. The aqueous layer was extracted twice with CH_2Cl_2, and the combined organic layer was washed with brine and dried over Na_2SO_4. Removal of the solvent under vacuum left a residue. The crude product was purified by column chromatography on silica gel with hexane/dichloromethane (5:1) to give, after removal of the solvent, a white solid (1.2 g, 15%). ^{1}H NMR ($CDCl_3$, 300 MHz, ppm): δ 8.57−8.39 (9H, m), 7.91−7.86 (4H, m), 7.78−7.76(2H, m), 7.68−7.66 (2H, m), 7.64−7.34(15, m), 3.05−2.82 (18H, m), 2.31−1.99 (18H, m), 0.96−0.39 (198H, m). Elem anal. calcd (%) for $C_{189}H_{266}$: C, 89.44; H, 10.56. Found: C, 89.23; H, 10.41.

TruP. A solution of aldehyde **2** (1.2 g, 1.4 mmol) and pyrrole (0.10 g, 1.4 mmol) in dry CH_2Cl_2 (112 mL) was degassed for 30 min at room temperature in the dark. The condensation was initiated by the addition of $BF_3{\cdot}Et_2O$ in CH_2Cl_2 (15 μL). After stirring overnight, 2,3-dichloro-5,6-dicyano-1,4-benzoquinone (DDQ; 1.5 g, 2.3 mmol) was added. The reaction mixture was stirred for an additional 2 h. After the addition of triethylamine (1.0 mL), the reaction was stirred for 45 min, and the reaction was concentrated and chromatographed on silica gel using CH_2Cl_2/pentane (1:5) to obtain a purple solid (0.24 g, 20%). ^{1}H NMR ($CDCl_3$, 300 MHz, ppm): δ 9.05−9.03 (8H, m), 8.76−8.74 (4H, m), 8.45−8.29 (16H, m), 7.54−7.32 (24H, m), 3.22−2.99 (24H, m), 2.25−2.10 (24H, m), 0.98−0.56 (264H, m), −2.44 (2H, s). ^{13}C NMR ($CDCl_3$, 75 MHz, ppm): δ 154.0, 153.9, 152.5, 145.5, 140.6, 140.5, 140.5, 140.2, 138.96, 138.9, 138.5, 133.3, 131.6, 129.0, 126.7, 126.3, 125.0, 123.0, 122.5, 121.0, 56.2, 56.1, 56.1, 37.3, 31.8, 30.0, 29.8, 24.5, 24.2, 22.6, 22.5, 14.2, 14.2. MALDI-TOF MS, m/z calcd for $C_{272}H_{366}N_4$, m/z: 3688.88. Found (MH^+): 3691.913. Elem anal. calcd (%) for $C_{272}H_{366}N_4$: C, 88.49; H, 9.99; N, 1.52. Found: C, 88.27; H, 9.69. N, 1.58.

TruZnP. The free base porphyrin **TruP** (1.1 g, 0.30 mmol) was dissolved in THF (20 mL), and the solution was purged with nitrogen for 10 min. A solution of $Zn(OAc)_2$ (0.10 g, 0.45 mmol) in MeOH (10 mL) was added to the porphyrin solution, and the reaction mixture was stirred overnight. The solvents were removed under vacuum conditions leaving a purple solid, which was dissolved in CH_2Cl_2 and washed successively with 3 successive aliquots of 5% aqueous $NaHCO_3$. The organic layer was dried over $MgSO_4$, and the solvent was removed. The metalloporphyrin was obtained in excellent (close to quantitative) yield following silica gel chromatography with CH_2Cl_2/pentane (1:5)

to obtain a purple solid (1.1 g, 95%). ^{1}H NMR ($CDCl_3$, 300 MHz, ppm): δ 9.17−9.15 (8H, m), 8.77−8.74 (4H, m), 8.45−8.30 (16H, m), 7.55−7.37 (24H, m), 3.25−3.02 (24H, m), 2.22−2.11 (24H, m), 1.03−0.56 (264H, m). ^{13}C NMR ($CDCl_3$, 75 MHz, ppm): δ 153.7, 152.1, 150.5, 145.3, 145.2, 140.8, 140.4, 140.3, 139.8, 138.7, 138.6, 138.3, 132.8, 132.6, 132.2, 128.7, 126.5, 126.1, 124.8, 123.0, 122.7, 122.7, 122.3, 121.9, 55.9, 55.9, 55.8, 37.1, 31.6, 29.6, 24.5, 24.3, 24.0, 22.3, 22.2, 14.0, 13.9. MALDI-TOF MS, m/z calcd for $ZnC_{272}H_{364}N_4$: 3750.79. Found: 3753.620 (MH^+). Elem anal. calcd (%) for $C_{272}H_{364}N_4 + H_2O$: C, 86.58; H, 9.78; N, 1.48. Found: C, 86.37; H, 9.73. N, 1.45.

TriTruP (yield, 10%): The synthetic procedure was the same to that for **TruP**. ^{1}H NMR ($CDCl_3$, 400 MHz, ppm): δ 9.18 (8H, s), 8.82 (4H, s), 8.57−8.33 (40H, m), 7.90−7.84 (32H, m), 7.44−7.34 (48H, m), 3.34−2.97 (72H, m), 2.04−1.21 (72H, m), 1.21−0.46 (792H, m), −2.40 (2H, s). ^{13}C NMR ($CDCl_3$, 100 MHz, ppm): 154.8, 153.9, 152.5, 146.2, 146.1, 145.9, 145.8, 145.6, 145.3, 145.1, 145.05, 145.6, 140.0, 39.4, 139.1, 138.7, 138.3, 126.6, 126.2, 125.3, 124.9, 122.4, 121.1, 120.5, 56.3, 56.1, 55.9, 37.3, 31.9, 31.8, 31.7, 29.9, 29.8, 24.2, 22.6, 22.6, 22.5, 14.3, 14.2, 14.2. MALDI-TOF MS, m/z calcd for $C_{776}H_{1070}N_4$, m/z: 10446.39. Found: 10445.663 (MH^+). Elem anal. calcd (%) for $C_{776}H_{1070}N_4$: C, 89.15; H, 10.32; N, 0.54. Found: C, 89.37; H, 10.41; N, 0.61.

TriTruZnP (yield, 97%): The synthetic procedure is the same as that for **TruZnP**. ^{1}H NMR ($CDCl_3$, 400 MHz, ppm): δ 9.24 (8H, s), 8.85 (4H, s), 8.60−8.39 (40H, m), 7.93−7.87 (32H, m), 7.45−7.38 (48H, m), 3.45−2.83 (72H, m), 2.45−2.09 (72H, m), 1.23−0.51 (792H, m). ^{13}C NMR ($CDCl_3$, 100 MHz, ppm): 154.8, 153.8, 152.5, 145.9, 145.8, 145.6, 145.4, 145.1, 145.1, 140.6, 140.3, 140.0, 139.4, 139.1, 138.7, 138.3, 126.6, 126.2, 125.2, 124.9, 122.4, 120.4, 56.3, 56.3, 56.1, 55.9, 37.3, 37.2, 31.9, 31.8, 31.7, 30.0, 29.9, 29.7, 29.6, 24.4, 24.2, 24.1, 22.6, 22.5, 22.4, 14.3, 14.2, 14.1. MALDI-TOF MS, m/z calcd for $ZnC_{776}H_{1068}N_4$, m/z: 10508.30. Found: 10509.023 (M^+). Elem anal. calcd (%) for $ZnC_{774}H_{1068}N_4$: C, 88.61; H, 10.23; N, 0.53. Found: C, 88.57; H, 10.35; N, 0.55.

RESULTS AND DISCUSSION

Synthesis. The synthetic routes used to prepare the target dendrimers are presented in Scheme 1. A monobrominated derivative of 5,5,10,10,15,15-hexa-*n*-hexyltruxene was lithiated using *n*-butyllithium, quenched with trimethyl borate solution, and then acid hydrolyzed to produce the boronic acid **4**. Treatment of **1** with *n*-butyllithium, followed by the addition of DMF at −78 °C and hydrolysis, gives **3** in moderate yield. Compound **3** is easily separated and purified via flash chromatography. **TruP** is obtained from **3** and pyrrole using a conventional procedure.[32] The Suzuki coupling reaction between **4** and **3**, using $Pd(PPh_3)_4$ as a catalyst, proceeds smoothly to yield the dendritic compound **5**. Compound **7** can be obtained by a Suzuki coupling reaction between **6** and **4**.

Scheme 1. The Synthetic Routes of Truxene-Based Porphyrins

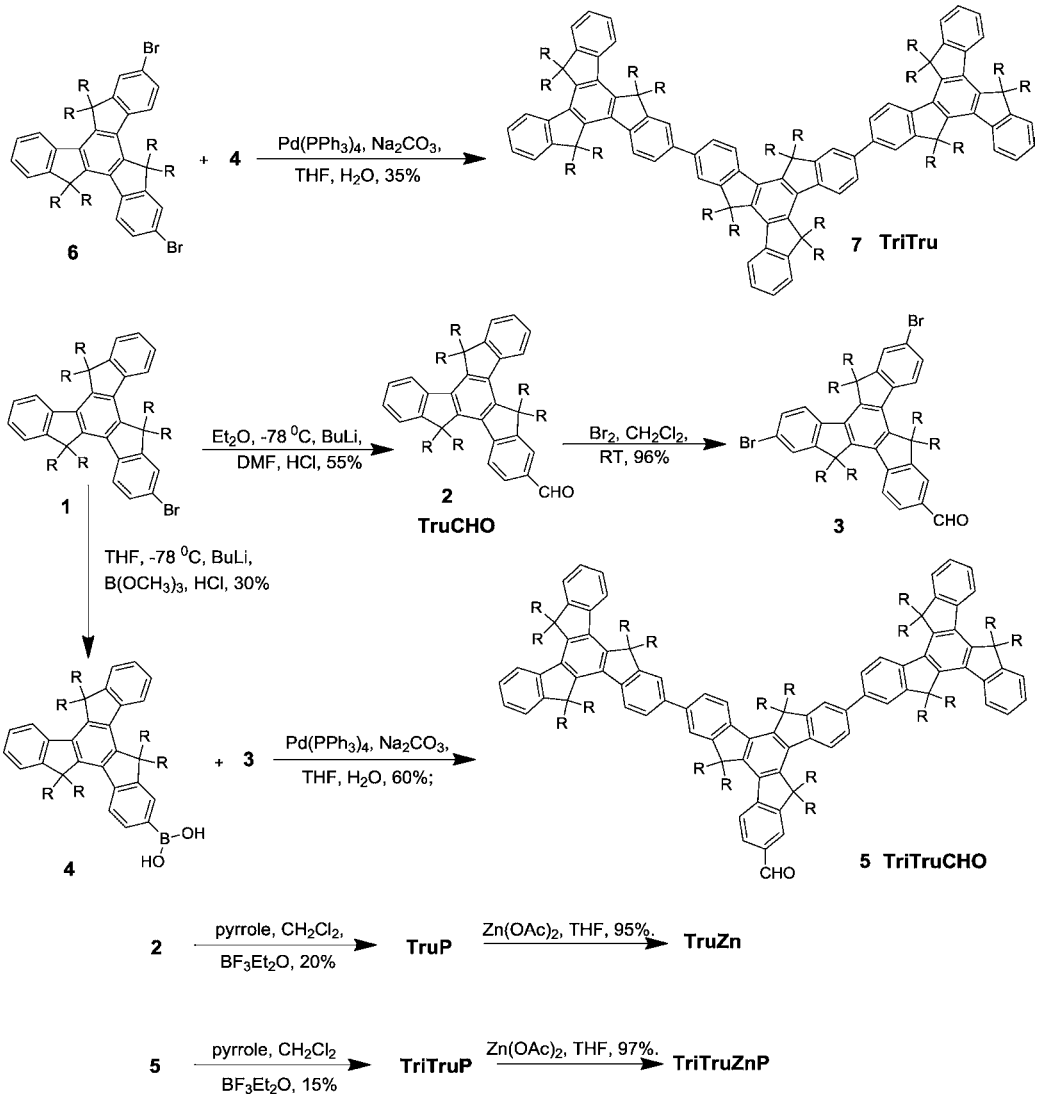

dx.doi.org/10.1021/ic2013667 | Inorg. Chem. 2011, 50, 11493−11505

TriTruP is synthesized by the same procedure to produce **TruP**. The synthesized porphyrins were characterized by MALDI-TOF-MS and ^{1}H and ^{13}C NMR. As anticipated, all compounds were soluble in common organic solvents, such as THF, hexane, $CHCl_3$, and toluene, owing to the large number of hexyl groups on the truxene units. **TriTruP** and **TriTruZnP** exhibit sharp and symmetrical elution patterns, with polydispersities (M_w/M_n) less than 1.02 (see Figure S22 of the Supporting Information, SI). The MALDI-TOF-MS spectra of the dendrimers also confirmed their monodispersity.

Spectroscopic and Photophysical Properties. The absorption spectra of truxene (**Tru**) and **TriTru** exhibit intense absorption bands in the UV region (Figure 1 and Table 1).

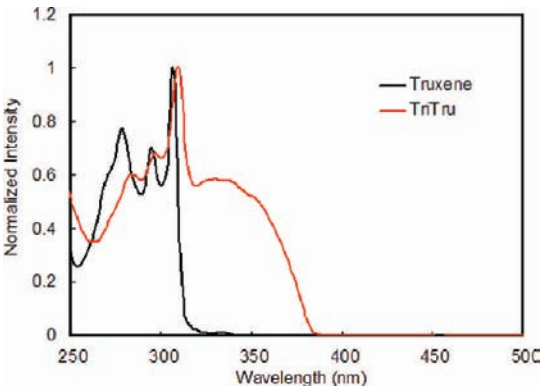

Figure 1. Absorption spectra of truxene and **TriTru** (2MeTHF, 298 K).

Table 1. UV−Vis Absorption Data for All Precursers and Target Dyads in 2MeTHF at 298 K

	λ_{abs}(nm) ($\varepsilon \times 10^{-3}$ M^{-1} cm^{-1})[a]		
compound	truxene	Soret	Q
Tru	278(36.1), 294(36.9), 306(55.6)		
TriTru	310(148.4), 350(79.1)		
TruP	296(103.2), 308(127.8)	428(339.1)	518(14.2), 556(12.6), 600(3.4), 653(4.3)
TriTruP	296(291.2), 308(425.3), 348(470.3)	429(613.9)	518(24.1), 558(23.5), 599(7.5), 653(9.1)
TruZnP	296(164.1), 308(178.3)	432(178.2)	520(3.9), 560(23.5), 603(16.3)
TriTruZnP	308(408.2), 350(448.1)	431(648.5)	560(31.7), 602(24.7)

[a]The absorption band is assigned to the truxene (**Tru**), the phorphyrin, or zinc(II) porphyrin (Soret band and Q band).

The narrow band at about 310 nm is present for both compounds and is due to a truxene-centered $\pi-\pi^*$ transiton.[9] **TriTru** exhibits a new, strong, red-shifted feature in the 320−380 nm range, which is also attributed to a $\pi-\pi^*$ transition and is associated with an increased conjugation in comparison with **Tru**.

The emission spectra of truxene exhibit a fluorescence band with some vibronic structure at 298 K and a strong phosphorescence band at 77 K with detailed vibronic structure starting at 457 nm (Figure 2). These spectra resemble those previously reported for truxene-related derivatives.[33] The **TriTru** fluorescence band is red-shifted (Figure 2), consistent with its absorption spectrum relative to that of truxene. **TriTru**

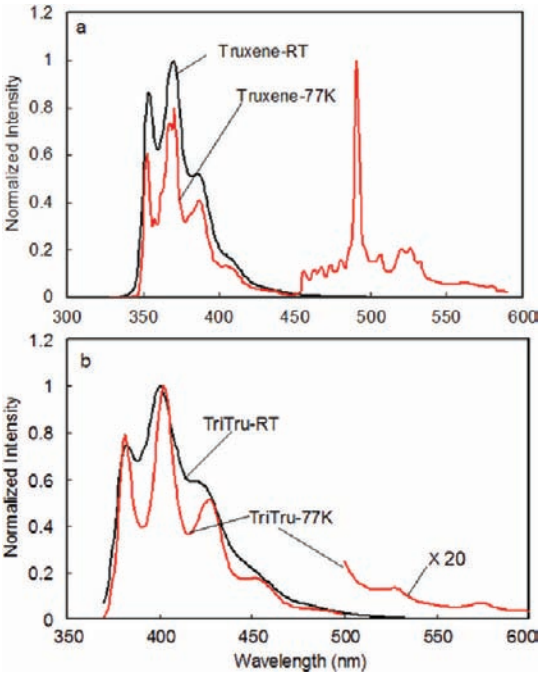

Figure 2. (a) Corrected emission spectra of truxene and of (b) **TriTru** at 298 and 77 K in 2MeTHF using λ_{exc}= 310 nm.

exhibits a weak phosphorescence with vibronic bands at 527 and 570 nm that differ in band shape and position compared with those of truxene. The emission data are listed in Table 2. The absorption and emission spectra of **TruCHO** and **TriTruCHO** are provided in the SI.

The absorption spectra of the porphyrin-containing materials exhibit the expected intense Soret band at ∼430 nm and the weaker Q-bands at longer wavelengths. The bands associated with the truxene units are detected below 400 nm where they are normally found (Figure 3, and the data are placed in Tables 1 and 2). Both the porphyrin absorption and luminescence bands (Figure 3) are red-shifted in comparison with those of the corresponding tetraphenylporphyrin free base and the corresponding zinc(II) complex (**H_2TPP** and **ZnTPP**).

The shape and position of the Soret and Q bands of the free base porphyrin and zinc(II) porphyrin (for example, **TruP** and **TriTruP**) remain unaffected whether the truxene or tritruxene is present (Figure 3 and Table 1). In addition, the emission maximum arising from the porphyrin and zinc(II) porphyrin are almost the same, implying that the tritruxene branch has little influence on the conjugation relative to monotruxene. Furthermore, with the increase in the number of truxene units, the absorptivity of the truxene-based unit in the 300−400 nm window increases, as expected, for the tritruxene materials, suggesting more effective light harvesting ability.

Interestingly, the fluorescence quantum yields (Φ_F) of the porphyrin fluorophore excited in the Q bands are 0.20 and 0.16 for **TruP** and **TriTruP** and 0.080 and 0.10 for **TruZnP** and **TriTruZnP** at 298 K, respectively. The Φ_F values are larger than those for **H_2TPP** (0.10) and **ZnTPP** (0.033), respectively.[23a] The increase of quantum efficiency in comparison with those of **TPP** and **ZnTPP** may result from a decrease in the "loose bolt effect" or "free rotor effect" of the substituent going from phenyl to truxene and tritruxene, which ultimately decrease the rate constant for internal conversion, k_{ic}. The motion likely to deactivate the excited state is the

dx.doi.org/10.1021/ic2013667 | Inorg. Chem. 2011, 50, 11493−11505

Table 2. Emission Data for All Precursors and Target Dyads in 2MeTHF

compound	chrom[a]	λ_{em}(nm)[b] 298 K	λ_{em}(nm) 77 K	Φ_F[c] 298 K
Tru	**Tru**	354, 370, 388	353, 377, 388, 407, 457, 463, 468, 474, 481, 491, 507, 522, 565, 581	*d*
TriTru	**Tru**	359, 376, 392, 412	357, 374, 395, 462, 465, 471, 478, 496, 502, 518, 538	*d*
TruP	**Tru**	356, 383, 404, 442		0.20
	P	661, 729	661, 729	
TriTruP	**Tru**	382, 425, 452	381, 424, 452, 473, 525	0.16
	P	661, 702	659, 701	
TruZnP	**Tru**	443	443,	0.076
	P	612, 663, 795	612, 663, 805	
TriTruZnP	**Tru**	382, 425, 452	382, 425, 452,	0.11
	P	612, 662	611, 662, 798	

[a]**Tru:** chromophore = truxene; **P**: chromophore = the phorphyrin or zinc(II) porphyrin. [b]The emission spectra was recorded using λ_{exc} = 310 nm under the inert atmosphere at 298 K. [c]Fluorescence quantum yields (Φ_F) of the samples in 2MeTHF were measured by using tetraphenylporphyrin and zinc-tetraphenylporphyrin (**H_2TPP**, Φ_F = 0.10 in THF; **ZnTPP**, Φ_F = 0.033 in THF) as standards.[23] [d]Not measured.

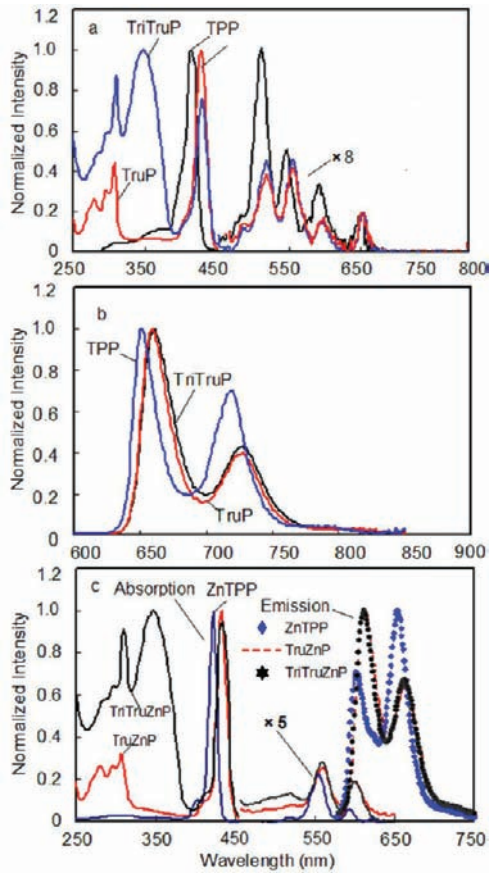

Figure 3. (a and b) Corrected absorption and emission spectra of **TPP**, **TruP**, and **TriTruP** in 2MeTHF at 298 K. (c) Corrected absorption and emission spectra of **ZnTPP**, **TruZnP**, and **TriTruZnP** in 2MeTHF at 298 K. λ_{exc}= 520 and 560 nm, for the free base and zinc(II) porphyrins, respectively.

low-frequency torsional mode where the *ortho*-H's of the phenyl groups come in contact with the prophyrin center. In the truxene and tritruxene cases, steric hindrance arising from intertruxene and -tritruxene hexyl−hexyl interactions prevent these aromatics from freely rotating.[23b] From a kinetic stand point, this would mean that k_{ic} decreases drastically upon the use of truxenes as substituents and that k_{ic} is of comparable size to the intersystem crossing rate constant, k_{isc}, which is unknown in this family of compounds. So, we provide this explanation to explain the increase in Φ_F with some reserve.

Molecular Orbital Analysis. The nature of the frontier MOs, electronic transitions, and lowest energy excited states were modeled using DFT (B3LYP) and TDDFT methods. The frontier MO representations are shown in Figure 4. The HOMO−2, HOMO, LUMO, and LUMO+1 orbitals exhibit the basic sets of π and π^* MOs located on the zinc(II) porphyrin central chromophore. The atomic contribution arising from the truxene aromatics onto these porphyrin-centered MOs is minimal or absent, confirming the weak conjugation effect in the band shifts observed in the absorption spectra. The HOMO−1 is a metal-centered $d_{x^2-y^2}$ interacting with the N lone pair in an antibonding fashion (see the Supporting Information) and does not contribute to the observed intensity in the absorption spectra.

The next four filled (HOMO−3 to HOMO−6) and empty MOs (LUMO+2 to LUMO+5) are centered on the truxenes, again with essentially no atomic contribution from the central porphyrin unit. This result suggests that these two different chromophores, truxene and porphyrine, are not strongly coupled. Evidence for this conclusion comes from the TDDFT computed electronic transitions (Table 3). In this table, the first 20 electronic transitions are listed, and the two sets of two degenerate lowest energy transitions that give rise to the Q and Soret bands are depicted.

These transitions, labeled #1 to #4, are computed at 520 (Q-band) and 395 nm (Soret band), which are blue-shifted with respect to the experimental values of 603 and 432 nm, respectively. This calculated blue shift relative to experimental values has previously been observed for other porphyrin systems[34] and thus can be corrected for. As a result, the calculations provide transition data appropriate for the scope of this work. The computed oscillator strength, *f*, is also in line with the observed relative intensity. More importantly, electronic transitions from the lower energy MOs, notably HOMO−3 to HOMO−6 (located on the truxene), and LUMO to LUMO+1 (located on the porphyrin) represent most of the electronic transitions between transition #5 and #20 (Table 3). The calculated *f* values ($0 < f < 0.0006$) are at least 2 orders of magnitude smaller than those computed for the Q band ($f \sim 0.057$). This is perfectly consistent with the very poor orbital overlap between the truxene and porphyrin chromophores (Figure 4). The truxene-localized electronic transitions from HOMO−3—HOMO−6 and LUMO+2—LUMO+5 are computed to appear at 310 nm, as experimentally observed, with *f* values that are 10 times weaker than those of the Q bands.

dx.doi.org/10.1021/ic2013667 | *Inorg. Chem.* 2011, 50, 11493–11505

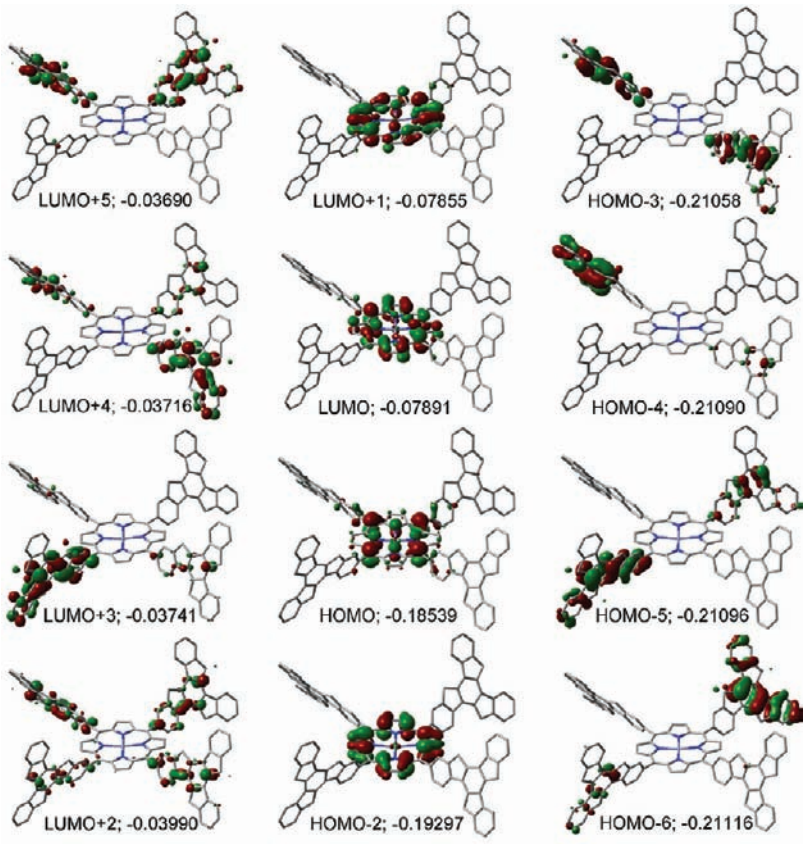

Figure 4. MO representations of the frontier MOs for **TruZnP** (from LUMO+5 to HOMO−6; the HOMO−1 is placed in the Supporting Information). The geometry of **TruZnP** was first optimized using the 6-31G* basis sets for Zn, C, N, and H, and the hexyl groups were removed for these calculations to save computation time. The energies are in au, and the dihedral angle formed by the truxene and porphyrin planes is 66.1°.

Table 3. Selected Computed (TDDFT) Positions of the 0−0 Electronic Transitions for TruZnP

no.	ν (cm^{-1})	λ (nm)	f	major contributions (%)
1	19227	520	0.0572	H−1→L+1 (36), HOMO→LUMO (61)
2	19228	520	0.0565	H−1→LUMO (36), HOMO→L+1 (61)
3	25296	395	1.1017	H−9→LUMO (35), H−8→LUMO (11), H−1→L+1 (26), HOMO→LUMO (18)
4	25300	395	1.0951	H-9→L+1 (35), H−8→L+1 (11), H−1→LUMO (26), HOMO→L+1 (18)
5	25685	389	0	H-7→L+1 (43), H−6→LUMO (45)
6	25787	388	0.0006	H−7→LUMO (22), H-7→L+1 (26), H−6→LUMO (26), H−6→L+1 (22)
7	25956	385	0.0001	H−7→LUMO (27), H−7→L+1 (22), H−6→LUMO (22), H−6→L+1 (25)
10	26053	384	0	H−7→LUMO (44), H−6→L+1 (45)
13	26453	378	0.0005	H−5→LUMO (14), H−3→LUMO (28), H−2→LUMO (47)
14	26455	378	0.0004	H−5→LUMO (29), H−4→LUMO (39), H−3→LUMO (23)
15	26457	378	0.0006	H-5→L+1 (15), H−3→L+1 (34), H−2→L+1 (43)
16	26458	378	0.0005	H−5→L+1 (33), H−4→L+1 (50)
17	26584	376	0.0001	H−3→LUMO (39), H−2→LUMO (44)
18	26585	376	0.0002	H−5→LUMO (43), H−4→LUMO (47)
19	26586	376	0.0001	H-5→L+1 (10), H−3→L+1 (34), H−2→L+1 (48)
20	26587	376	0.0002	H−5→L+1 (36), H−4→L+1 (42), H−3→L+1 (15)
41	32194	311	0.0013	H−7→L+9 (12), H−5→L+2 (11)
42	32197	311	0.0048	H−6→L+8 (12), H−3→L+4 (10)
43	32198	311	0.0054	H−5→L+3 (12), HOMO→L+9 (12)
44	32201	311	0.0054	H−5→L+4 (10), HOMO→L+8 (12)

dx.doi.org/10.1021/ic2013667 | *Inorg. Chem.* 2011, 50, 11493–11505

An approximated absorption spectrum can be generated by tracing the bar graph of the electronic transitions as a function of f (green lines in Figure 5) and assigning a thickness (red line). This is an approximation since no vibronic coupling is taken into account.

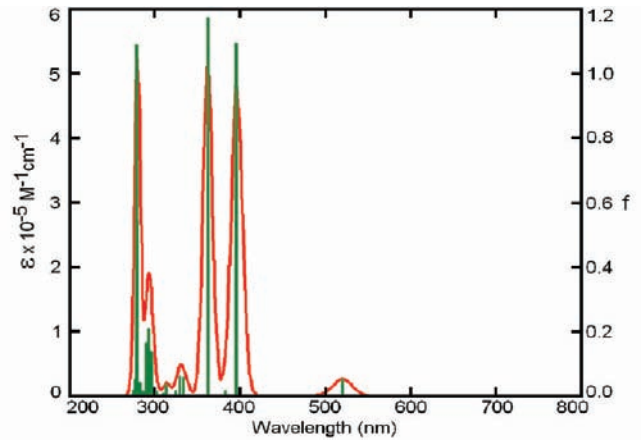

Figure 5. Computed UV–vis spectrum of **TruZnP** by TDDFT.

Evidence for Singlet and Triplet Energy Transfer in Truxene-Containing Porphyrins. Absorption and emission data indicate that the truxene- and porphyrin-based chromophores are the energy donor and acceptor, respectively. Excitation at 310 nm, where the truxene absorbs most strongly, leads to a decrease in intensity of the fluorescence and phosphorescence arising from truxene in the dyads, whereas the luminescence from the free base or zinc(II) porphyrin unit remains strong. These quenchings appear to be a consequence of singlet and triplet energy transfers. This suggestion is supported by the transient absorption measurements shown below, where only T_1-T_n transient absorption bands of the porphyrins are detected, thus excluding the possibility of excited state quenching by photoinduced electron transfers.

For **TruP** and **TriTruP**, the truxene-based luminescence is almost absent at 298 K (Figure 6a), whereas the remaining truxene donor emissions at 382 and 443 nm arising from **TruZnP** and **TriTruZnP** are very weak (Figure 6b and c). In all cases, the origins of the emission bands were confirmed by comparing the absorption and excitation spectra. The excitation spectra monitored in the porphyrin fluorescence at 298 K (λ_{max}= 660 for **TruP** and **TriTruP** and 615 nm for **TruZnP** and **TriTruZnP**) overlaps well with the combined absorptions of the truxene unit and the porphyrin core (SI), indicating further energy transfer.

ZnTPP is known to show a phosphorescence at 780 nm in rigid glasses at 77 K,[35] but such an emission from zinc(II) porphyrins has scarcely been observed at 298 K. In this work, a phosphorescence at 793 nm at 298 K is noted for **TruZnP** (Figure 6b). Two reasons may explain this behavior. The presence of the hexyl groups may hinder the rotation about the porphyrin–truxene *meso*-C–C single bond, as described above ("*loose bolt effect*" or "*free rotor effect*" applied to the porphyrin chromophore), thus decreasing intramolecular collision with the aryl *ortho*-H. These hexyl groups can also decrease the solvent–chromophore interactions (intermolecular collisions), thus decreasing the nonradiative decay rate constants $T_1 \rightarrow S_0$. Additionally, truxene to porphyrin triplet–triplet energy transfer can increase the porphyrin triplet state population if excited in the truxene-based excited states.

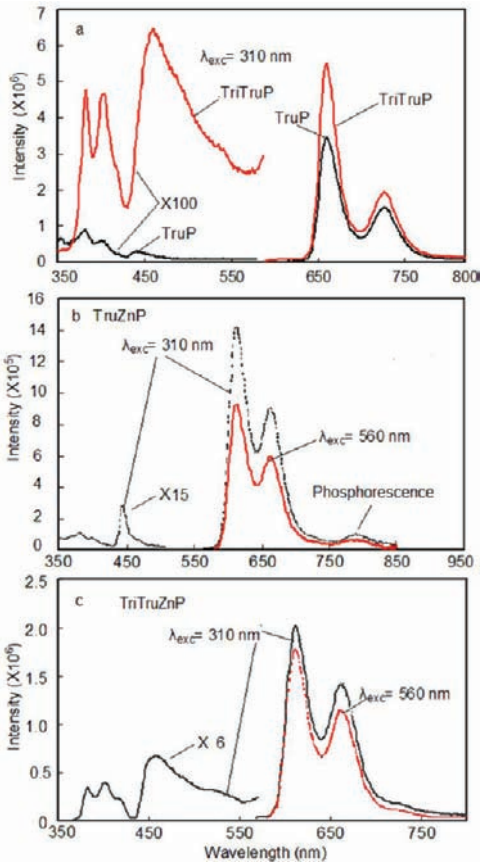

Figure 6. Corrected emission spectra of the porphyrin free bases (1.5×10^{-6} M) (a) and zinc(II) porphyrins (b and c) (5×10^{-6} M) at 298 K.

Phosphorescence arising from the zinc(II) porphyrin unit at 77 K (λ_{exc} = 560 nm; i.e., Q-band) is observed (Figure 7a). Relevant to this energy transfer study, the phosphorescence peaks are at 802 and 798 nm for **TruZnP** and **TriTruZnP**, respectively, which represent a red-shift relative to **ZnTPP** (780 nm). The difference between for **TruZnP** and **TriTruZnP** (i.e., 4 nm) indicates that the larger tritruxene unit must have a less extensive π-conjugation between the truxene and porphyrine planes. This is most likely due to a difference in dihedral angle between the truxene and porphyrine planes (in **TriTruZnP**) toward 90°, thus decreasing the π conjugation. For **TruZnP** and **TriTruZnP** at 77 K, the usually strong truxene fluorescence and phosphorescence are observed, but they are much weaker (λ_{exc} = 310 nm), indicating obvious quenching (Figure 7b). **TruP** and **TriTruP** exhibit noticeable energy transfer at 77 K, and the emission intensity of the free base chromophore of **TriTruP** increases, after the excitation at donor absorption (at 310 nm), relative to **TruP** (Figure 7c). Moreover, there is a significant increase in the zinc(II) porphyrin fluorescence and phosphorescence intensity (λ_{exc}= 310 nm) as compared to the intensity when λ_{exc}= 560 nm (Figure 7d). In addition, the excitation spectra monitored at these porphyrin-centered phosphorescence bands exhibit bands arising from both the truxene and porphyrin units, providing further evidence for triplet energy transfer (see the SI). Triplet energy transfer from the truxene donor to the acceptor (porphyrin or zinc(II) prophyrin) can also contribute to the increase of the fluorescence and phosphorescence intensity of the acceptor,

dx.doi.org/10.1021/ic2013667 | *Inorg. Chem.* 2011, 50, 11493–11505

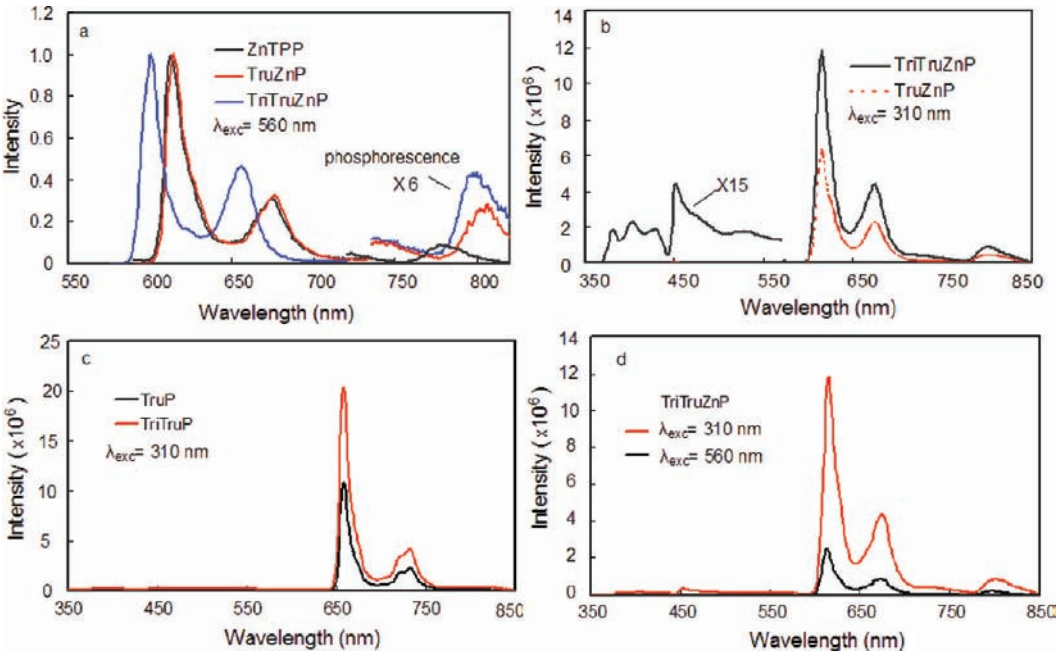

Figure 7. Comparison of the emission spectra of free-base porphyrins (1.5×10^{-6} M) and zinc(II) porphyrins (5×10^{-6} M) at 77 K, excited at different wavelengths.

as illustrated in Figure 8. The singlet−singlet energy transfer from S_1(**Tru**) to S_1(**P**) and S_1(**ZnP**) or to S_2(**P**) to S_2(**ZnP**) is possible, but we cannot distinguished between them in this work.[36]

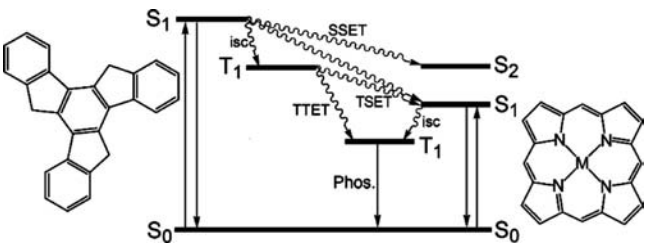

Figure 8. State diagram representing the different fragments involved in the energy transfer processes in this work. **Phos.**, phosphorescence; **SSET**, singlet−singlet energy transfer; **TTET**, triplet−triplet energy transfer; **TSET**, triplet−singlet energy transfer; **ISC**, intersystem crossing.

All photophysical data for the porphyrin free base and zinc(II) porphyrin chromophores are listed in Tables 4 and 5 and are typical for these kinds of chromophores.

The triplet state energy of the zinc(II) porphyrins is lower relative to that of truxenes on the basis of the phosphorescence spectra (Figures 2 and 7), so triplet truxene→porphyrin energy transfers are possible. The triplet−triplet absorption spectra (T_1−T_n) for truxene and **TruZnP** are shown in Figure 9, and the lifetime data are listed in Table 5. The **TruZnP** T_1−T_n absorption spectra show transient absorptions centered at 480 and 750 nm, which are very similar to those for **ZnTPP**,[37] indicating that these species lie in their triplet states. No evidence for a charge separated state was observed in this work. However, the truxene T_1−T_n absorption centered at 580 nm is not observed for **TruZnP**, meaning that the triplet sate of the truxene unit is either depopulated in the dendrimers (the T_1−T_n absorption spectra of **TriTruZnP** exhibit the same behavior) or buried under stronger transient absorptions of the porphyrin chromophore. The transient absorption traces decay monoexponentially with lifetimes of 1.9 and 3.9 ms for **TruZnP** and **TriTruZnP**, respectively. The τ_P of **TruZnP** and **TriTruZnP** is 25 and 43 ms at 805 nm at 77 K, respectively, which are typical for triplet lifetimes for zinc(II) porphyrins.

Rate Constants for Singlet and Triplet Energy Transfer in Truxene-Containing Porphyrins. The singlet−singlet energy transfer rate (k_{ET}) is given by $k_{ET} = (1/\tau_F) - (1/\tau_F^o)$,[21] where τ_F and τ_F^o are the fluorescence lifetimes of the donor in the presence and absence of the acceptor, respectively. In the **TruZnP** and **TruP** cases, truxene is used as a comparison species, and the k_{ET} data are listed in Table 4. At 298 K, the singlet k_{ET} values are 1.2 and 5.9 $(ns)^{-1}$ for **TruZnP** and **TruP**, respectively. At 77 K, these are 2.6 $(ns)^{-1}$ for both **TruZnP** and **TruP**. In the **TriTruZnP** and **TriTruP** cases, **TriTru** is used as a comparison species, and the k_{ET} values are 0.74 and 0.87 $(ns)^{-1}$ for **TriTruZnP** and **TriTruP** at 298 K and 1.2 and 2.7 $(ns)^{-1}$ for **TriTruZnP** and **TriTruP** at 77 K, respectively. The small rate variation between 298 and 77 K may be due to a small geometry change, namely, for the dihedral angle between the average truxene and porphyrin planes. These rates are considered efficient but moderate when compared to other multiporphyrin assemblies.[21]

The dipole−dipole interaction (Förster) and exchange (Dexter) mechanisms are assumed to be operative in the singlet−singlet energy transfers.[38] **TruZnP** is used as an example for the possibility of the Dexter process. The calculated dihedral angle between the average truxene and porphyrin planes averages 66.1° (optimized geometry computed by DFT), so the orbital overlap is weak, consistent with the relatively modest red-shift of the absorption (Soret and Q bands) and emission bands going from **ZnTPP** to **TruZnP**. This fact greatly diminishes the possibility of a Dexter exchange mechanism, in which spatial orbital overlap is necessary. The poorer orbital overlap will lead to the slower singlet−singlet energy transfer rate arising from the Dexter mechanism.[6b] Moreover, because

dx.doi.org/10.1021/ic2013667 | Inorg. Chem. 2011, 50, 11493–11505

Table 4. Fluorescence Lifetime and Singlet−Singlet Energy Transfer Rate Constants

		298 K			77 K		
compound	chromo[a]	τ_F (ns)[b]	λ_{em} (nm)[b]	k_{ET} (ns)$^{-1}$ 298 K	τ_F (ns)[b]	λ_{em} (nm),[b]	k_{ET} (ns)$^{-1}$ 77 K
truxene	**Tru**	56.26 ± 0.15	380(310)		64.64 ± 0.52	380(310)	
TriTru	**Tru**	2.87 ± 0.13	380(310)		3.81 ± 0.06	380(310)	
TruP	**P**	12.18 ± 0.11	660(520)		10.07 ± 0.35	660(520)	
	Tru	0.17 ± 0.03	380(310)	5.9	0.38 ± 0.04	380(310)	2.6
TriTruP	**P**	12.81 ± 0.28	660(520)		13.91 ± 1.43	660(520)	
	Tru	1.12 ± 0.02	380(310)	0.87	0.36 ± 0.02	380(310)	2.7
TruZnP	**P**	1.68 ± 0.02	615(560)		2.25 ± 0.03	615(560)	
	Tru	0.80 ± 0.03	380(310)	1.2	0.39 ± 0.06	380(310)	2.6
TriTruZnP	**P**	1.68 ± 0.04	615(560)		1.98 ± 0.02	615(560)	
	Tru	1.32 ± 0.02	380(310)	0.74	0.82 ± 0.02	380(310)	1.2

[a]**Tru**: chromophore = truxene; **P**: chromophore = the phorphyrin or zinc(II) porphyrin. [b]The lifetimes were recorded under an inert atmosphere, and the values in parentheses indicate at which wavelength the samples were excited (2MeTHF).

Table 5. Phosphorescence Lifetimes and Triplet Energy Transfer Rate Constants of the Truxene−Porphyrin Dendrimers in 2MeTHF at 77 K and Triplet−Triplet Transient Lifetimes at 298 K

		lifetime, 77 K			transient lifetime, 298 K	
compound	chromo.[a]	τ_p(ms)	λ_{em}(nm) [b]	k_{ET} (ms)$^{-1}$ 77 K	(T_1-T_n) τ_{trans}(ms)[d]	λ_{abs}(nm) [c]
Truxene	**Tru**	620.2 ± 0.3	490		0.040	580
TriTru	**Tru**	212.4 ± 8.5	490		*e*	*e*
TruP	**Tru**	0.51 ± 0.03	480		*e*	*e*
TriTruP	**Tru**	35.3 ± 2.9	480		*e*	*e*
TruZnP	**Tru**	0.71 ± 0.04	480	1.3	1.9	500
	P	25.0 ± 0.4	800			
TriTruZnP	**Tru**	80.3 ± 6.7	480	0.01	3.9	500
	P	43.2 ± 0.1	800			

[a]**Tru**: chromophore = truxene; **P**: chromophore = the phorphyrin or zinc(II) porphyrin. [b]The lifetime was recorded from the emission wavelength under the inert atmosphere. [c]The recorded absorption wavelength. [d]The lifetimes were recorded at the absorption maximum at 298 K in degassed 2MeTHF. [e]No signal.

the critical distance at which the Dexter process is dominant (i.e., below 5 Å) is known, then the Dexter mechanism will dominate the energy transfer, rather than the Förster resonance energy transfer mechanism.[38] In our case, the distance between donor and acceptor is very small, and the Dexter process should, in principle, dominate the singlet−singlet energy transfer, but for the fact that the orbital overlap is poor.

The Förster process must also be considered. The relative orientation of the transition moments of the two chromophores plays a major role in the amplitude of the rate according to Förster theory.[22b,c] The orientation factor term, κ^2, takes a maximum value (4) when the dipole transition moments are parallel and is minimal (0) when perpendicular. Generally, the κ^2 (2/3) is often assumed for random orientations.[22b,c] Lower κ^2 values lead to slower energy transfer rates. In these molecular systems, the truxene or tritruxene units are not expected to rotate freely due to steric hindrance arising from large aryl groups and long hexyl chains. A space filling model and a scheme showing the relative orientations of the planar transition moments of the two chromophores are shown in Figures 10 and 11, respectively. The κ^2 term (not calculated here) will strongly depend on the dihedral angle (~66°) but is expected to be weak.

In addition, unlike chlorophylls, truxene is practically a nonpolar substituent (as well as the porphyrin central chromophore), so the dipole transition moments are very small. The Förster rate constant is further bound to be lower. Finally, the integral overlap between the emission spectrum of the donor and the absorption spectrum of the acceptor is an important factor which affects the singlet energy transfer rate. From Figures 2 and 3, the spectral overlap between the emission spectrum of truxene and the absorption spectrum of porphyrin, the (J) intergral in Förster theory, is very weak, which will result in the slower rate. In conclusion, it is highly likely that both the Förster and Dexter mechanisms operate, but in both cases several structural parameters contribute to reduce the singlet−singlet energy transfer rate constants. The fact that rates of medium amplitudes are recorded is fully consistent with the structural parameters.

Experimentally, there is no gain in rate constant going from the truxene to the tritruxene antenna. The measured rates are all on the same order of magnitude, and it appears that all of the work is being mainly performed by the closest truxene to the porphyrin. This means that the truxene units in tritruxene remotely placed from the porphyrin center have very little effect. This contrasts with several works that report that the larger dendrimers can provide more channels for the dissipation of excitation energy despite a greater average distance from the peripheral donors to the central acceptors.[39] The reason for this difference most likely stems from the flexibility of the dendrons providing favorable orientations and distance for energy migration across the dendrimers. This is not the case here as the dendrons are relatively rigid. However, one may speculate that the flexible *n*-hexyls of truxene and tritruxene may induce a "*loose bolt effect*" or "*free rotor effect*" rapidly draining the excited state population of the truxene chromophore by nonradiative pathways (intersystem crossing from the triplet manifold) down to the ground state ($T_1 \rightarrow S_0$). Because there are

dx.doi.org/10.1021/ic2013667 | *Inorg. Chem.* 2011, 50, 11493–11505

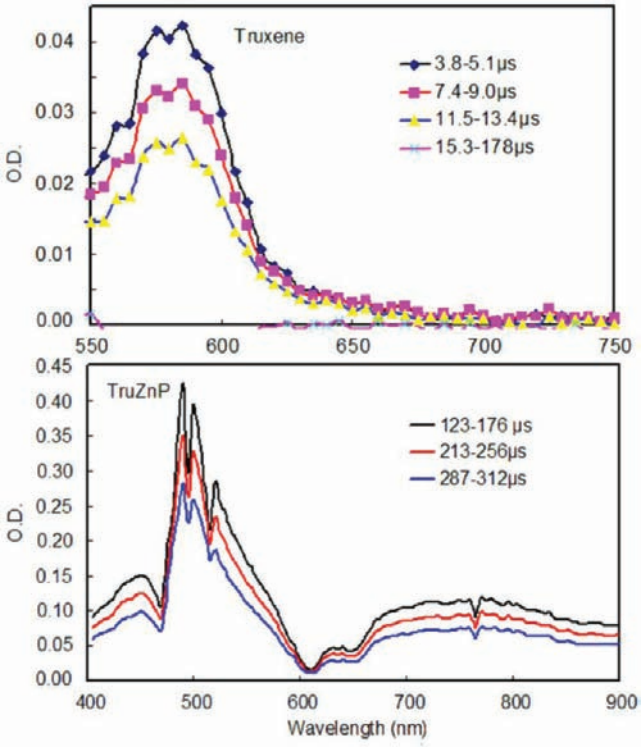

Figure 9. The transient absorption spectra of truxene and **TruZnP** at 298 K in degassed 2MeTHF. λ_{exc}= 355 nm, and the delay times are indicated inside the graphs.

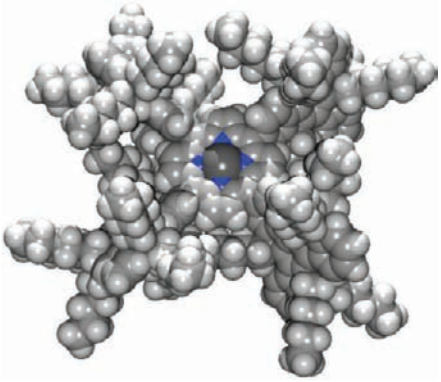

Figure 10. Space filling model of **TruZnP** (optimized geometry; DFT).

more *n*-hexyl groups in tritruxene than in truxene, the rate for nonradiative relaxation may be faster in the former, resulting in low probability of energy transfer. In other words, the benefit of absorbing more photons in the tritruxene is canceled out by having more flexible substituents on the donors deactivating the excited states.

The triplet k_{ET} values at 77 K are also extracted as 1.3×10^3 s^{-1} and 0.10×10^2 s^{-1} for **TruZnP** and **TriTruZnP** at 77 K, respectively. While these triplet−triplet k_{ET} values compare with those of other triplet energy transfer systems, these values lie on the very lower end of the literature data.[21,40,41] Owing to the fact that triplet excited states are of the radical type, dipole driven Förster processes do not occur, so only the Dexter mechanism operates.[40,42] For the same orbital overlap arguments presented above, the triplet k_{ET} is also expected to be slow, as experimentally observed.

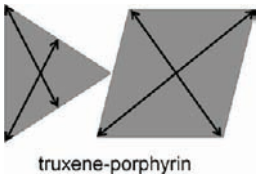

Figure 11. Schematic representation of the dipole transition moments (black arrows) in the truxene (triangle) relative to porphyrin (square). Only one truxene is shown for simplicity.

As for a possible reason why one truxene substituent leads to a faster triplet energy transfer (in comparison with the tritruxene substituent), one may again speculate that the multiple and flexible *n*-hexyl side chains of tritruxene (in comparison with truxene) may induce a "loose bolt" effect,[15,23] rapidly decreasing the triplet excited state population by nonradiative pathways (intersystem crossing $T_1 \rightarrow S_0$).

CONCLUSION

Four soluble porphyrins functionalized with truxenes were prepared, and spectral evidence for efficient singlet−singlet energy transfers from the truxenes to the porphyrin core have been observed. The rates are indeed efficient but are average when compared to other multiporphyrin assemblies.[23] There is also no advantage in adding truxene units on the antennae, where both the singlet and triplet k_{ET} either stay the same or slightly decrease when replacing the truxene antennae by tritruxenes. The triplet energy transfer rates at 77 K (Dexter mechanism) are very slow, which is likely due to a poor orbital overlap between the truxene and porphyrin π systems as corroborated by DFT calculations. Interestingly, the increase in fluorescence quantum yields of the free base and zinc(II) porphyrin chromophores in the dendrimers in comparison with parent **H_2TPP** and **ZnTPP**, using an excitation wavelength in the Q region (i.e., away from the donor bands), and the appearance of a phosphorescence of the free base and zinc(II) chromophores at 298 K indicate a decrease in nonradiative rate constants (internal conversion, $S_1 \rightarrow S_0$, and intersystem crossing, $T_1 \rightarrow S_0$), probably associated with hexyl−hexyl interactions preventing free rotation about the porphyrin−truxene C−C bond.

ASSOCIATED CONTENT

Supporting Information

NMR and mass spectra; GPC and crystal structure; absorption, emission, and excitation spectra. This material is available free of charge via the Internet at http://pubs.acs.org.

AUTHOR INFORMATION

Corresponding Author

*Tel.: 001-819-821-7092. Fax: 001-819-821-8017. E-mail: Pierre.Harvey@USherbrooke.ca.

ACKNOWLEDGMENTS

This research was supported by the Natural Sciences and Engineering Research Council of Canada (NSERC), le Fonds Québécois de la Recherche sur la Nature et les Technologies (FQRNT), the Centre d'Etudes des Matériaux Optiques et Photoniques de l'Université de Sherbrooke (CEMOPUS), and the Agence National de la Recherche (ANR) for a grant of a Research Chair of Excellence.

REFERENCES

(1) (a) Wolffs, M.; Hoeben, F. J. M.; Beckers, E. H. A.; Schenning, A. P. H. J.; Meijer, E. W. *J. Am. Chem. Soc.* **2005**, *127*, 13484−13485. (b) Hoeben, F. J. M.; Wolffs, M.; Zhang, J.; De Feyter, S.; Leclere, P.; Schenning, A. P. H. J.; Meijer, E. W. *J. Am. Chem. Soc.* **2007**, *129*, 9819−9828.

(2) (a) Harth, E. M.; Hecht, S.; Helms, B.; Malmstrom, E. E.; Fréchet, J. M. J.; Hawker, C. J. *J. Am. Chem. Soc.* **2002**, *124*, 3926−3938. (b) Li, B.; Li, J.; Fu, Y.; Bo, Z. *J. Am. Chem. Soc.* **2004**, *126*, 3430−3431. (c) Fei, Z.; Li, B.; Bo, Z.; Lu, R. *Org. Lett.* **2004**, *6*, 4703−4706.

(3) (a) Kozaki, M.; Akita, K.; Suzuki, S.; Okada, K. *Org. Lett.* **2007**, *9*, 3315−3318. (b) Chng, L. L.; Chang, C. J.; Nocera, D. G. *Org. Lett.* **2003**, *5*, 2421−2424. (c) Kozaki, M.; Akita, K.; Okada, K. 2007, *9*, 1509-1512.

(4) (a) Harriman, A. Energy transfer in synthetic porphyrin arrays. In *Supramolecular Photochemistry*; Balzani, V., Ed.; D. Reidel Publishing Company: Dordrecht, Holland, 1987; pp 207−223. (b) Gust, D.; Moore, T. A.; Moore, A. L. *Acc. Chem. Res.* **1993**, *26*, 198−205. (c) Terazono, Y.; Kodis, G.; Liddell, P. A.; Garg, V.; Moore, T. A.; Moore, A. L.; Gust, D. *J. Phys. Chem. B.* **2009**, *113*, 7147−7155. (d) Seth, J.; Palaniappan, V.; Wagner, R. W.; Johnson, T. E.; Lindsey, J. S.; Bocian, D. F. *J. Am. Chem. Soc.* **1996**, *118*, 11194−11207. (e) Kuciauskas, D.; Liddell, P. A.; Lin, S.; Johnson, T. E.; Weghorn, S. J.; Lindsey, J. S.; Moore, A. L.; Moore, T. A.; Gust, D. *J. Am. Chem. Soc.* **1999**, *121*, 8604−8614. (f) Ikemoto, J.; Takimiya, K.; Aso, Y.; Otsubo, T.; Fujitsuka, M.; Ito, O. *Org. Lett.* **2002**, *4*, 309−311. (g) Imaoka, T.; Horiguchi, H.; Yamamoto, K. *J. Am. Chem. Soc.* **2003**, *125*, 340−341. (h) Loiseau, F.; Campagna, S.; Hameurlaine, A.; Dehaen, W. *J. Am. Chem. Soc.* **2005**, *127*, 11352−11363. (g) Kimura, M.; Shiba, T.; Yamazaki, M.; Hanabusa, K.; Shirai, H.; Kobayashi, N. *J. Am. Chem. Soc.* **2001**, *123*, 5636−5642.

(5) (a) Oliva, M. M.; Casado, J.; López Navarrete, J. T.; Berridge, R.; Skabara, P. J.; Kanibolotsky, A. L.; Perepichka, I. F. *J. Phys. Chem. B.* **2007**, *111*, 4026−4035. (b) Gómez-Lor, B.; de Frutos, Ó.; Ceballos, P. A.; Granier, T.; Echavarren, A. M. *Eur. J. Org. Chem.* **2001**, 2107−2114. (c) Abdourazak, A. H.; Marcinow, Z.; Sygula, A.; Sygula, R.; Rabideau, P. W. *J. Am. Chem. Soc.* **1995**, *117*, 6410−6411. (d) Gómez-Lor, B.; Gonzalez-Cantalapiedra, E.; Ruiz, M.; de Frutos, Ó.; Cárdenas, D. J.; Santos, A.; Echavarren, A. M. *Chem.—Eur. J.* **2004**, *10*, 2601−2608.

(6) (a) Diring, S.; Puntoriero, F.; Nastasi, F.; Campagna, S.; Ziessel, R. *J. Am. Chem. Soc.* **2009**, *131*, 6108−6110. (b) Chan, C. K. M.; Tao, C.-H.; Tam, H.-L.; Zhu, N. Y.; Yam, V. W-W.; Cheah, K.-W. *Inorg. Chem.* **2009**, *48*, 2855−2864.

(7) (a) Wang, J.-L.; Yan, J.; Tang, Z.-M.; Xiao, Q.; Ma, Y. G.; Pei, J. *J. Am. Chem. Soc.* **2008**, *130*, 9952−9962. (b) Ventura, B.; Barbieri, A.; Barigelletti, F.; Diring, S.; Ziessel, R. *Inorg. Chem.* **2010**, *49*, 8333−8346.

(8) (a) Wang, J.-L.; Luo, J.; Liu, L.-H.; Zhou, Q.-F.; Ma, Y.; Pei, J. *Org. Lett.* **2006**, *8*, 2281−2284. (b) Jiang, Y.; Lu, Y.-X.; Cui, Y.-X.; Zhou, Q.-F.; Ma, Y.; Pei, J. *Org. Lett.* **2007**, *9*, 4539−4542.

(9) (a) Pei, J.; Wang, J.-L.; Cao, X.-Y.; Zhou, X.-H.; Zhang, W.-B. *J. Am. Chem. Soc.* **2003**, *125*, 9944−9945. (b) Sun, Y.; Xiao, K.; Liu, Y.; Wang, J.-L.; Pei, J.; Yu, G.; Zhu, D. *Adv. Funct. Mater.* **2005**, *15*, 818−822. (c) Wang, J.-L.; Duan, X.-F.; Jiang, B.; Gan, L.-B.; Pei, J.; He, C.; Li, Y.-F. *J. Org. Chem.* **2006**, *71*, 4400−4410.

(10) (a) Yang, J.-S.; Lee, Y.-R.; Yan, J.-L.; Lu, M.-C. *Org. Lett.* **2006**, *8*, 5813−5816. (b) Yang, J.-S.; Huang, H.-H.; Ho, J.-H. *J. Phys. Chem. B* **2008**, *112*, 8871−8878.

(11) (a) Yang, J.-S.; Huang, H.-H.; Liu, Y.-H.; Peng, S.-M. *Org. Lett.* **2009**, *11*, 4942−4945. (b) Yang, J.-S.; Huang, H.-H.; Lin, S.-H. *J. Org. Chem.* **2009**, *74*, 3974−3977.

(12) (a) Kreyenschmidt, M.; Klaerner, G.; Fuhrer, T.; Aschenhurst, J.; Karg, S.; Chen, W. D.; Lee, V. Y.; Scott, J. C.; Miller, R. D. *Macromolecules* **1998**, *31*, 1099−1103. (b) Montgomery, N. A.; Denis, J.-C.; Schumacher, S.; Ruseckas, A.; Skabara, P. J.; Kanibolotsky, A.; Paterson, M. J.; Galbraith, I.; Turnbull, G. A.; Samuel, I. D.W. *J. Phys. Chem. A.* **2011**, *115*, 2913−2919.

(13) (a) Schmidt-Mende, L.; Fechtenkötter, A.; Müllen, K.; Moons, E.; Friend, R. H.; MacKenzie, J. D. *Science* **2001**, *293*, 1119−1122. (c) Wiesler, U. M.; Berresheim, A. J.; Morgenroth, F.; Lieser, G.; Müllen, K. *Macromolecules* **2001**, *34*, 187−199.

(14) Gagnon, K.; Aly, S. M.; Wittmeyer, A. B.; Bellows, D.; Bérubé, J. F.; Caron, L.; Abd-El-Aziz, A. S.; Fortin, D.; Harvey, P. D. *Organometallics* **2008**, *27*, 2201−2214.

(15) Liu, L.; Fortin, D.; Harvey, P. D. *Inorg. Chem.* **2009**, *48*, 5891−5900.

(16) Jiang, F.-L.; Fortin, D.; Harvey, P. D. *Inorg. Chem.* **2010**, *49*, 2614−2623.

(17) (a) Xu, T.; Lu, R.; Jin, M.; Qiu, X.; Xue, P.; Bao, C.; Zhao, Y. *Tetrahedron Lett.* **2005**, *46*, 6883−6886. (b) Xu, T.; Lu, R.; Qiu, X.; Liu, X.; Xue, P.; Tan, C.; Bao, C.; Zhao, Y. *Eur. J. Org. Chem.* **2006**, 4014−4020.

(18) (a) Zheng, Q.; He, G. S.; Prasad, P. N. *Chem. Mater.* **2005**, *17*, 6004−6011. (b) Pei, J.; Wang, J.-L.; Cao, X.-Y.; Zhou, X.-H.; Zhang, W.-B. *J. Am. Chem. Soc.* **2003**, *125*, 9944−9945. (c) Kanibolotsky, A. L.; Berrifge, R.; Skabara, P. J.; Perepichka, I. F.; Bradley, D. D. C.; Koeberg, M. *J. Am. Chem. Soc.* **2004**, *126*, 13695−13702. (d) Wang, L.; Jiang, Y.; Luo, J.; Zhou, Y.; Zhou, J. H.; Wang, J.; Pei, J. *Adv. Mater.* **2009**, *47*, 4854−4858.

(19) (a) Cao, X.-Y.; Liu, X.-H.; Zhou, X.-H.; Zhang, Y.; Jiang, Y.; Cao, Y.; Cui, Y.-X.; Pei, J. *J. Org. Chem.* **2004**, *69*, 6050−6058.

(20) Duan, X. F.; Wang, J. L.; Pei, J. *Org. Lett.* **2005**, *7*, 4071−4073.

(21) Harvey, P. In *Porphyrin Handbook*; Kadish, K. M., Smith, K. M., Guilard, R., Eds.; Academic Press: Boston, 2003; Vol. *18*, p 63.

(22) (a) Harvey, P. D.; Stern, C.; Guilard, R. In *Handbook of Porphyrin Science With Applications to Chemistry, Physics, Materials Science, Engineering, Biology and Medicine*; Kadish, K. M., Smith, K. M., Guilard, R., Eds.; World Scientific Publishing: Singapore, 2011; pp 1−179. (b) Förster, T. *Ann. Phys.* **1948**, *2*, 55−73. (c) Förster, T. *Naturwissenschaften* **1946**, *33*, 166−175.

(23) (a) Aly, S. M.; Ayed, C.; Stern, C.; Guilard, R.; Abd-El-Aziz, A. S.; Harvey, P. D. *Inorg. Chem.* **2008**, *47*, 9930−9940. (b) Loutfy, R. O.; Law, K. Y. *J. Phys. Chem.* **1980**, *84*, 2803−2808.

(24) Frisch, M. J.et al. *Gaussian 09(1)*; Gaussian, Inc.: Wallingford, CT, 2004.

(25) (a) Becke, A. D. *J. Chem. Phys.* **1993**, *98*, 5648−5652. (b) Lee, C.; Yang, W.; Parr, R. G. *Phys. Rev. B* **1988**, *37*, 785−789. (c) Miehlich.; Savin, A.; Stoll, H.; Preuss, H. *Chem. Phys. Lett.* **1989**, *157*, 200−206.

(26) (a) Binkley, J. S.; Pople, J. A.; Hehre, W. J. *J. Am. Chem. Soc.* **1980**, *102*, 939−947. (b) Gordon, M. S.; Binkley, J. S.; Pople, J. A.; Pietro, W. J.; Hehre, W. J. *J. Am. Chem. Soc.* **1982**, *104*, 2797−2803. (c) Pietro, W. J.; Francl, M. M.; Hehre, W. J.; Defrees, D. J.; Pople, J. A.; Binkley, J. S. *J. Am. Chem. Soc.* **1982**, *104*, 5039−5048. (d) Dobbs, K. D.; Hehre, W. J. *J. Comput. Chem.* **1986**, *7*, 359−378. (e) Dobbs, K. D.; Hehre, W. J. *J. Comput. Chem.* **1987**, *8*, 861−879. (f) Dobbs, K. D.; Hehre, W. J. *J. Comput. Chem.* **1987**, *8*, 880−893.

(27) Stewart, J. J. P. *J. Mol. Model* **2007**, *13*, 173−213.

(28) (a) Hohenberg, P.; Kohn, W. *Phys. Rev.* **1964**, *136*, B864−871. (b) Kohn, W.; Sham, L. J. *Phys. Rev.* **1965**, *140*, A1133−1138. (c) Salahub, D. R.; Zerner, M. C. *The Challenge of d and f Electrons*; American Chemical Society: Washington, DC, 1989. (d) Parr, R. G.; Yang, W. *Density-Functional Theory of Atoms and Molecules*; Oxford Univ. Press: Oxford, U. K., 1989.

(29) (a) Stratmann, R. E.; Scuseria, G. E.; Frisch, M. J. *J. Chem. Phys.* **1998**, *109*, 8218−8224. (b) Bauernschmitt, R.; Ahlrichs, R. *Chem. Phys. Lett.* **1996**, *256*, 454−464. (c) Casida, M. E.; Jamorski, C.; Casida, K. C.; Salahub, D. R. *J. Chem. Phys.* **1998**, *108*, 4439−4449.

(30) O'Boyle, N. M.; Tenderholt, A. L.; Langner., K. M. *J. Comput. Chem.* **2008**, *29*, 839−845.

(31) (a) Jiang, Y.; Lu, Y. X.; Cui, Y. X.; Zhou, Q. F.; Ma, Y. G.; Pei., J *Org. Lett.* **2007**, *9*, 4539−4541. (b) Cao, X. Y.; Zhang, W; Zi, H.; Pei., J. *Org. Lett.* **2004**, *6*, 4845−4848.

(32) (a) Lindsey, J. S.; Schreiman, I. C.; Hsu, H. C.; Kearney, P. C.; Marguerettaz, A. M. *J. Org. Chem.* **1987**, *52*, 827−836. (b) Vollmer, M. S.; Würthner, F.; Effenberger, F.; Emele, P.; Meyer, D. U.; Stümpfig, T.; Port, H.; Wolf, H. C. *Chem.—Eur. J.* **1998**, *4*, 260−269.

(33) Baunsgaard, D.; Harrit, N.; El Balsami, M.; Negri, F.; Orlandi, G.; Frederiksen, J.; Wilbrandt, R. *J. Phys. Chem. A* **1998**, *102*, 10007–10016.
(34) (a) Jiang, F. L.; Fortin, D.; Harvey., P. D. *Inorg. Chem.* **2010**, *49*, 2614–2623. (b) Bellows, D.; Aly, S. M.; Goudreault, T.; Fortin, D.; Gros, C. P.; Barbe, J.-M.; Harvey, P. D. *Organometallics* **2010**, *29*, 317–325.
(35) Rozhkov, V. V.; Khajehpour, M.; Vinogradov, S. A. *Inorg. Chem.* **2003**, *42*, 4253–4258.
(36) Vollmer, M. S.; Effenberger, F.; Stümpfig, T.; Hartschuh, A.; Port, H.; Wolf, H. C. *J. Org. Chem.* **1998**, *63*, 5080–5087.
(37) Nojiri, T.; Watanabe, A.; Ito, O. *J. Phys. Chem. A.* **1998**, *102*, 5215–5219.
(38) Faure, S.; Stern, C.; Guilard, R.; Harvey, P. D. *J. Am. Chem. Soc.* **2004**, *126*, 1253–1261.
(39) Devadoss, C.; Bharathi, P.; Moore, J. S. *J. Am. Chem. Soc.* **1996**, *118*, 9635–9644.
(40) Faure, S.; Stern, C.; Espinosa, E.; Guilard, R.; Harvey, P. D. *Chem.—Eur. J.* **2005**, *11*, 3469–3472.
(41) Aly, S. M.; Ho, C.-L.; Fortin, D.; Wong, W.-Y.; Abd-El-Aziz, A. S.; Harvey, P. D. *Chem.—Eur. J.* **2008**, *14*, 8341–8352.
(42) Dexter, D. L. *J. Chem. Phys.* **1953**, *21*, 836–850.